Astronomy in Focus, XXIXB, Focus Meeting 22
XXIXth IAU General Assembly, August 2015
Piero Benvenuti, ed.

doi:10.1017/S1743921316006773

Spatially resolved spectroscopy of lensed galaxies in the Frontier Fields

Tucker Jones[1,2,3] and the GLASS collaboration[4]

[1]Institute for Astronomy, University of Hawaii at Manoa
Honolulu, HI 96822, USA
email: tucker.jones@hawaii.edu

[2]Department of Physics, University of California, Santa Barbara
Santa Barbara, CA 93106, USA

[3]Hubble Fellow

[4]http://glass.physics.ucsb.edu/

Abstract. The Grism Lens-Amplified Survey from Space (GLASS) has obtained slitless near-infrared spectroscopy of 10 galaxy clusters selected for their strong lensing properties, including all six Hubble Frontier Fields. Slitless grism spectra are ideal for mapping emission lines such as [O II], [O III], and Hα at $z = 1$–3. The combination of strong gravitational lensing and Hubble's diffraction limit provides excellent sensitivity with spatial resolution as fine as 100 pc for highly magnified sources, and ∼500 pc for less magnified sources near the edge of the field of view. The GLASS survey represents the largest spectroscopic sample with such high resolution at $z > 1$. GLASS and Hubble Frontier Field data provide the distribution of stellar mass, star formation, gas-phase metallicity, and other aspects of the physical structure of high redshift galaxies, reaching stellar masses as low as $\sim 10^7$ M$_\odot$ at $z = 2$. I discuss precise measurements of these physical properties and implications for galaxy evolution.

Keywords. gravitational lensing, galaxies: abundances, galaxies: evolution, galaxies: high-redshift

1. Introduction

Spatially resolved spectroscopy at the diffraction limit of large telescopes has led to tremendous advances in our understanding of how galaxies evolve at high redshifts. Progress has largely come from surveys of galaxies at $z \simeq 1$–3, the epoch at which cosmic star formation density peaks and the morphological Hubble sequence emerges. Spectral mapping of emission lines at near-infrared wavelengths reveals the kinematics and distribution of star formation, while multiple line ratios reveal the gas-phase metallicity (e.g., Jones *et al.* 2013). These data show a prominence of turbulent thick disks among the star forming population while roughly one third undergoing mergers at $z = 2$. Surveys of the largest and most massive galaxies have revealed kinematic settling toward lower redshifts, evidenced by decreasing merger fractions and disk velocity dispersion (e.g., Wisnioski *et al.* 2015). However, typical L* galaxies at $z \gtrsim 2$ have effective radii of only ∼2 kpc which are poorly sampled by current instruments and hence difficult to characterize. A promising solution is to observe gravitationally lensed galaxies with large areal magnification factors. Early results showed that lensing can be utilized to achieve physical resolution as fine as 100 pc (Nesvadba *et al.* 2006; Stark *et al.* 2008; Jones *et al.* 2010a), a tremendous advance over the ∼1 kpc resolution achieved with adaptive optics (AO) or with Hubble Space Telescope at near-infrared wavelengths.

Despite the gain in spatial resolution and sensitivity, relatively few lensed galaxies have been targeted with integral field spectrographs (∼30 to date at $z \simeq 2$: e.g., Jones *et al.*

2010a; Livermore *et al.* 2015; Leethochawalit *et al.* 2015). Nonetheless these surveys have made several important discoveries including the prevalence of thick disks in low-mass galaxies (previously thought to have little or no ordered rotation; Jones *et al.* 2010a), ubiquitous giant H II regions consistent with fragmentation from gravitational instability (Jones *et al.* 2010a; Livermore *et al.* 2012), and the first measurements of metallicity gradients at high redshift and their subsequent evolution (Jones *et al.* 2010b, 2013; Yuan *et al.* 2011). The kinematic properties of lensed galaxies are reasonably well established in the context of larger surveys at lower spatial resolution. Metallicity gradients are more challenging in that they are significantly underestimated in poorly-sampled data (Yuan *et al.* 2013; Leethochawalit *et al.* 2015). Early analyses showed negative gradient slopes suggesting inside-out disk growth and moderate star formation feedback (Jones *et al.* 2013). However, non-lensing studies found inverted gradients at high redshift, arguing for rapid "cold flow" accretion (Cresci *et al.* 2010; Queyrel *et al.* 2012). The lack of consensus is largely due to a scarcity of data. Securing adequate spatial resolution is challenging, as is finding lensed sources for which multiple emission lines can be mapped in practical integration times. The work presented here is concerned with using space-based grism spectroscopy to enlarge the sample of reliable metallicity gradients.

2. GLASS: Resolved Spectroscopy with the Hubble Space Telescope

The infrared grisms on Hubble's Wide Field Camera 3 (WFC3) obtain slitless spectroscopy at low spectral and high spatial resolution. This provides two-dimensional emission lines maps for all objects within WFC3's field of view. The Grism Lens-Amplified Survey from Space (GLASS) is obtaining grism spectra in the cores of 10 strong lensing galaxy clusters including all six Frontier Fields, with several scientific objectives. Treu *et al.* (2015) give a comprehensive overview of the survey. One goal is to study galaxy assembly and gas flows using spatially resolved emission line maps and derived metallicity (i.e., gas-phase oxygen abundance) in lensed galaxies. Hubble is well-suited to this application because of the broad spectral wavelength range (0.8–1.7 μm), near-unity Strehl ratio, wide field of view, and lack of sky lines or telluric absorption bands. In contrast, ground-based AO-fed instruments can observe only a single galaxy with a limited useful wavelength range and Strehl ratios of $\sim$0.2 at most. Figure 1 demonstrates the advantages of GLASS, showing results from three example galaxies at $z \simeq 1.9$ observed in a single pointing towards the cluster MACS 0717 (Jones *et al.* 2015). Extended line emission is detected in all three cases enabling spatially resolved metallicity measurements.

3. Metallicity Gradients and Global Properties

Figure 2 shows early results from GLASS in combination with previously reported measurements of metallicity gradients as well as integrated metallicity. Uncertainty in measurements derived from GLASS data is comparable and typically smaller than previous work at $z \simeq 2$, and extends to an order of magnitude lower in stellar mass (reaching $\sim 10^7\,\mathrm{M}_\odot$). This mass range is of particular interest as it corresponds to the regime where local dwarf galaxy properties are in tension with theoretical expectations. The initial results in Figure 2 support a picture whereby galaxy mergers and interactions result in flattened metallicity gradients, with lower overall gas-phase metallicity and hence more efficient feedback in lower-mass galaxies (Jones *et al.* 2015). Larger samples will reveal the effects of feedback on galaxy evolution based on metallicity gradient evolution, the mass-metallicity relation, and other diagnostics as well as through comparison with cosmological simulations (e.g., Figure 2; Gibson *et al.* 2013; Anglés-Alcázar *et al.* 2014).

https://doi.org/10.1017/S1743921316006773 Published online by Cambridge University Press

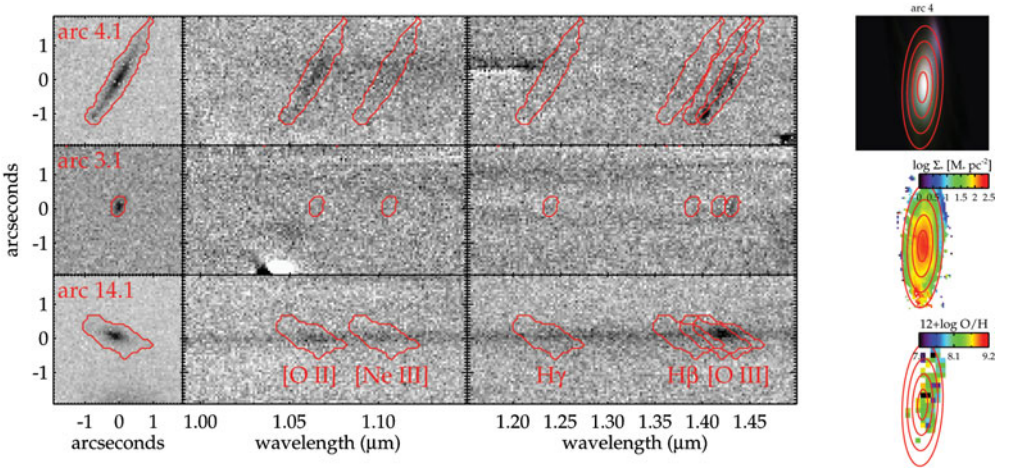

Figure 1. Hubble grism spectra and associated physical properties obtained as part of the GLASS survey. **Left.** Grism spectra of three lensed galaxies at $z \simeq 1.9$ observed in the same pointing. Two different grisms provide contiguous wavelength coverage from 0.8–1.7 μm, including multiple strong emission lines. Contours show the extracted spatial extent of each line. **Right.** Two-dimensional maps of properties derived for the source "arc 4," reconstructed in the image plane. Panels show the intrinsic morphology, stellar mass surface density, and gas-phase metallicity. Overlaid contours show constant de-projected galactocentric radius. *A color version of this figure is available online.*

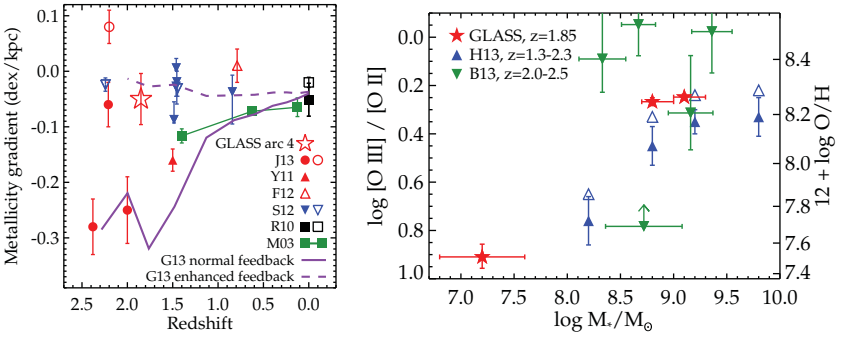

Figure 2. Left. The evolution of metallicity gradients with redshift. Measurements of gravitationally lensed galaxies with $\lesssim 300$ pc resolution are shown in red (GLASS arc 4: Jones *et al.* 2015; J13: Jones *et al.* 2013; Y11: Yuan *et al.* 2011; F12: Frye *et al.* 2012), non-lensed galaxies with $\sim$1 kpc resolution are shown in blue (S12: Swinbank *et al.* 2012), an average of local gradients are shown in black (R10: Rupke *et al.* 2010), and the Milky Way metallicity gradient evolution measured from planetary nebulae is shown in green (M03: Maciel *et al.* 2003). Solid and hollow symbols denote isolated disks and interacting (or merging) galaxies, respectively, demonstrating that interacting galaxies have flatter gradients on average in the lensed and $z = 0$ samples. We additionally show results of two different feedback schemes in otherwise identical simulations of a galaxy similar to those shown in this figure (G13: Gibson *et al.* 2013). Simulations suggest that stronger feedback leads to shallower gradients at high redshifts. **Right.** Mass-metallicity relation for lensed galaxies observed in GLASS and by Belli *et al.* (2013, B13), and composite spectra of non-lensed galaxies from Henry *et al.* (2013, H13). Galaxies at lower mass typically have lower metallicity and hence more efficient feedback. GLASS data extend previous work by an order of magnitude in stellar mass, probing the dwarf galaxy regime where strong feedback may substantially alter the central dark matter density (Jones *et al.* 2015). *A color version of this figure is available online.*

https://doi.org/10.1017/S1743921316006773 Published online by Cambridge University Press

4. Prospects for the Near Future

The results in Figure 2 are a proof of concept that GLASS delivers high quality measurements of integrated as well as spatially resolved metallicity, reaching low intrinsic flux and stellar mass limits. The survey is now complete and analysis is ongoing, with a paper in preparation by Wang *et al.* We expect to obtain approximately 20 gradient measurements and ∼100 integrated metallicity measurements with precision comparable to that in Figure 2. This will approximately double the number of well-measured gradients at $z \simeq 2$, accounting for the enlarged sample published by Leethochawalit *et al.* (2015) following this focus meeting. Ground-based followup of GLASS targets is also in progress to measure kinematic properties using KMOS on the Very Large Telescope. The statistical power from GLASS combined with prior samples will greatly improve inferences on the overall evolution of metallicity gradients, their relation to gas kinematics, and implications for the role of feedback and galactic-scale outflows.

Acknowledgements

It is a pleasure to thank the Frontier Field focus meeting organizers for all of their efforts. This contribution represents a culmination of work by numerous collaborators. Readers are referred to the relevant publications for more details, in particular: Jones *et al.* (2015); Treu *et al.* (2015), and the references cited herein.

References

Anglés-Alcázar, D., Davé, R., Özel, F., & Oppenheimer, B. D. 2014, *ApJ*, 782, 84
Belli, S., Jones, T., Ellis, R. S., & Richard, J. 2013, *ApJ*, 772, 141
Cresci, G., Mannucci, F., Maiolino, R., *et al.* 2010, *Nature*, 467, 811
Förster Schreiber, N. M., Genzel, R., Bouché, N., *et al.* 2009, *ApJ*, 706, 1364
Frye, B. L., Hurley, M., Bowen, D. V., *et al.* 2012, *ApJ*, 754, 17
Gibson, B. K., Pilkington, K., Brook, C. B., Stinson, G. S., & Bailin, J. 2013, *A&A*, 554, A47
Henry, A., Scarlata, C., Domínguez, A., *et al.* 2013, *ApJ*, 776, L27
Jones, T. A., Swinbank, A. M., Ellis, R. S., Richard, J., & Stark, D. P. 2010, *MNRAS*, 404, 1247
Jones, T., Ellis, R., Jullo, E., & Richard, J. 2010, *ApJ*, 725, L176
Jones, T., Ellis, R. S., Richard, J., & Jullo, E. 2013, *ApJ*, 765, 48
Jones, T., Wang, X., Schmidt, K. B., *et al.* 2015, *AJ*, 149, 107
Leethochawalit, N., Jones, T. A., Ellis, R. S., *et al.* 2015, *ApJ* submitted, arXiv:1509.01279
Livermore, R. C., Jones, T., Richard, J., *et al.* 2012, *MNRAS*, 427, 688
Livermore, R. C., Jones, T. A., Richard, J., *et al.* 2015, *MNRAS*, 450, 1812
Maciel, W. J., Costa, R. D. D., & Uchida, M. M. M. 2003, *A&A*, 397, 667
Nesvadba, N. P. H., Lehnert, M. D., Eisenhauer, F., *et al.* 2006, *ApJ*, 650, 661
Queyrel, J., Contini, T., Kissler-Patig, M., *et al.* 2012, *A&A*, 539, A93
Rupke, D. S. N., Kewley, L. J., & Chien, L.-H. 2010, *ApJ*, 723, 1255
Stark, D. P., Swinbank, A. M., Ellis, R. S., *et al.* 2008, *Nature*, 455, 775
Swinbank, A. M., Sobral, D., Smail, I., *et al.* 2012, *MNRAS*, 426, 935
Treu, T., Schmidt, K. B., Brammer, G. B., *et al.* 2015, *ApJ*, 812, 114
Wisnioski, E., Förster Schreiber, N. M., Wuyts, S., *et al.* 2015, *ApJ*, 799, 209
Yuan, T.-T., Kewley, L. J., Swinbank, A. M., *et al.* 2011, *ApJ*, 732, L14
Yuan, T.-T., Kewley, L. J., & Rich, J. 2013, *ApJ*, 767, 106